Supporting Information

Rare electron-transfer photochromic and thermochromic difunctional compounds

Pei-Xin Li,[a] Ming-Sheng Wang,*[a] Li-Zhen Cai,[a] Guan-E Wang[a] and Guo-Cong Guo*[a]

*State Key Laboratory of Structural Chemistry, Fujian Institute of Research on the Structure of Matter, Chinese Academy of Sciences, Fuzhou, Fujian 350002, P. R. China. *E-mail: gcguo@fjirsm.ac.cn (G.-C. Guo); mswang@fjirsm.ac.cn (M.-S. Wang)*

Materials. $ZnCl_2$, $ZnBr_2$, 4,4'-bipyridine, and 2-$BrCH_2COOH$ in AR grade were purchased commercially and used without further purification. Water was deionized and distilled before use. The ligand CEbpy was obtained as a hydrated compound CEbpy·$3H_2O$ according to the same procedure reported in the literature,[1] which showed the observable photoactive phenomena

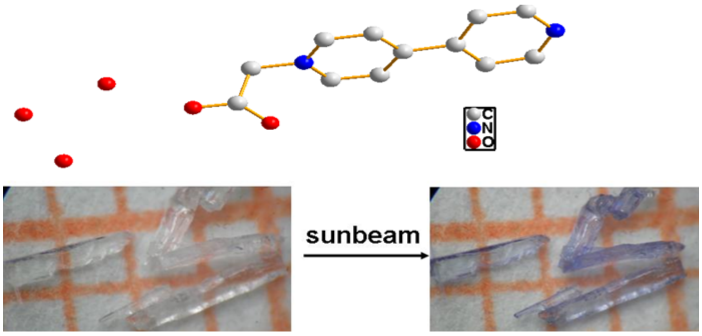

Fig. S1. The asymmetry unit of CEbpy·$3H_2O$ (top); the color of CEbpy·$3H_2O$ crystals turned to light blue under the sunbeam (bottom).

Determination.

A PLS-SXE300C 300 W xenon lamp system equipped with an IR filter was used to prepare colored samples, and the distances between these samples and the Xe lamp were around 30 cm.

UV−visible (UV−vis) spectra were recorded at room temperature on a PerkinElmer

Lambda 900 UV/vis/NIR spectrophotometer equipped with an integrating sphere in the wavelength range of 200−1200 nm. $BaSO_4$ plates were used as references (100% reflection), on which the finely ground power of each sample was coated. Powder X-ray diffraction (XRD) patterns were collected with a Rigaku MiniFlex II diffractometer powered at 30 kV and 15 mA for Cu $K\alpha$ (λ = 1.54056 Å). Simulated patterns were produced using the Mercury Version 1.4 software (http://www.ccdc.cam.ac.uk/products/mercury/) and single-crystal reflection diffraction data. Electron spin resonance (ESR) spectra were recorded on a Bruker ER-420 spectrometer with a 100 kHz magnetic field in the X band at room temperature.

X-ray Crystallographic Study. The X-ray diffraction measurement of **1**, **2, and 2T** were performed on a Rigaku SATURN70 CCD diffractometer using graphite monochromated Mo $K\alpha$ radiation (λ = 0.71073 Å). The primitive structures of **1**, **2**, and **2T** were solved by the direct method using the Siemens SHELXTL Version 5 package of crystallographic software.[2,3] Difference Fourier maps based on these atomic positions yielded other non-hydrogen atoms. The final structure was refined using a full-matrix least-squares refinement on F^2. All non-hydrogen atoms were refined anisotropically. The hydrogen atoms on carbon atoms were generated geometrically. Crystallographic data and structural refinements for the compounds are summarized in Table S1. Important bond distances are listed in Table S2 and S3. More details on the crystallographic studies as well as atomic displacement parameters are given as cif Supporting Information.

The entry of CCDC-994628-994630 and CCDC-1021644 contains the supplementary crystallographic data for **1** and **2**. These data can be obtained free of charge at http://www.ccdc.cam.ac.uk/conts/retrieving.html or from the Cambridge Crystallograp hic Dat a Centre, 12, Uni on Road, Cambridge CB2 1EZ, U.K. Fax: (Internet) +44-1223/336-033. E-mail: deposit@ccdc.cam.ac.uk

Syntheses of [ZnX_2(CEbpy)] (X = Cl, 1; Br, 2).

Compounds **1** and **2** were synthesized by the reaction of $ZnCl_2$ (27 mg, 0.2 mmol) or $ZnBr_2$ (45 mg, 0.2 mmol) and CEbpy·$3H_2O$ (53 mg, 0.2 mmol) in 20 mL of a water/ethanol (1/1 v/v) mixture. The solution was filtered and allowed to stand in the dark for several days to produce pale yellow and yellow block crystals for **1** and **2**, respectively. Yields based on Zn: 42% for **1**; 34% for **2**. The phase purities of their crystalline samples were checked by powder XRD (Fig. S2) and elemental analyses. Calcd (%) for **1**: C, 41.10; H, 2.88; N, 7.99. Found (%): C, 38.99; H, 2.87; N, 7.55. Calcd (%) for **2**: C, 32.80; H, 2.30; N, 6.38. Found (%): C, 32.99; H, 2.45; N, 6.54.

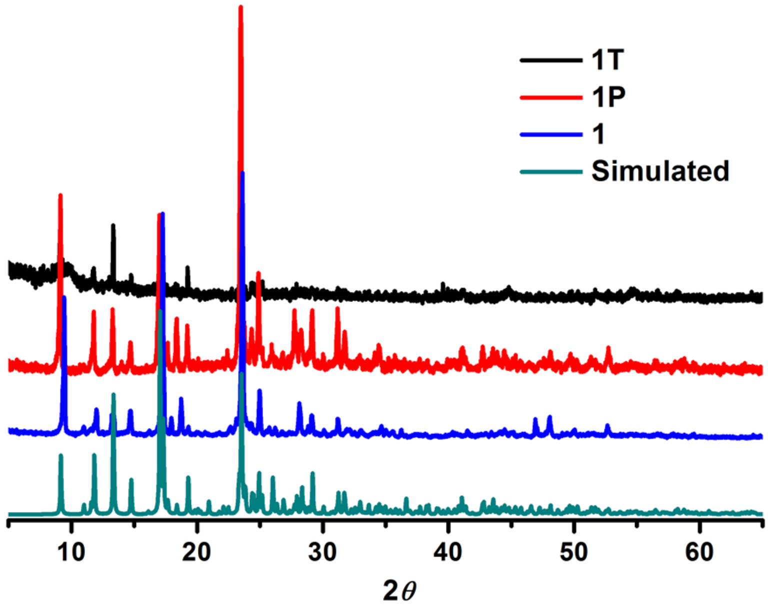

(a)

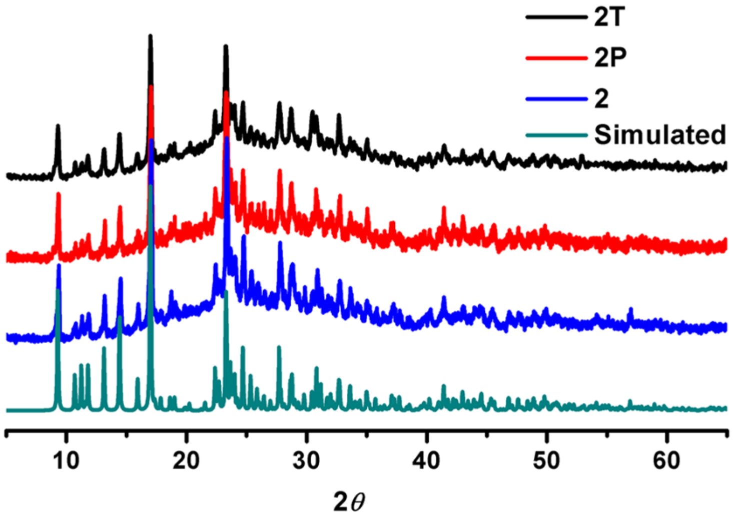

(b)

Fig. S2. Powder XRD patterns of **1** and **2** before and after the photo or thermo effects, and their simulated patterns from single-crystal X-ray structure data.

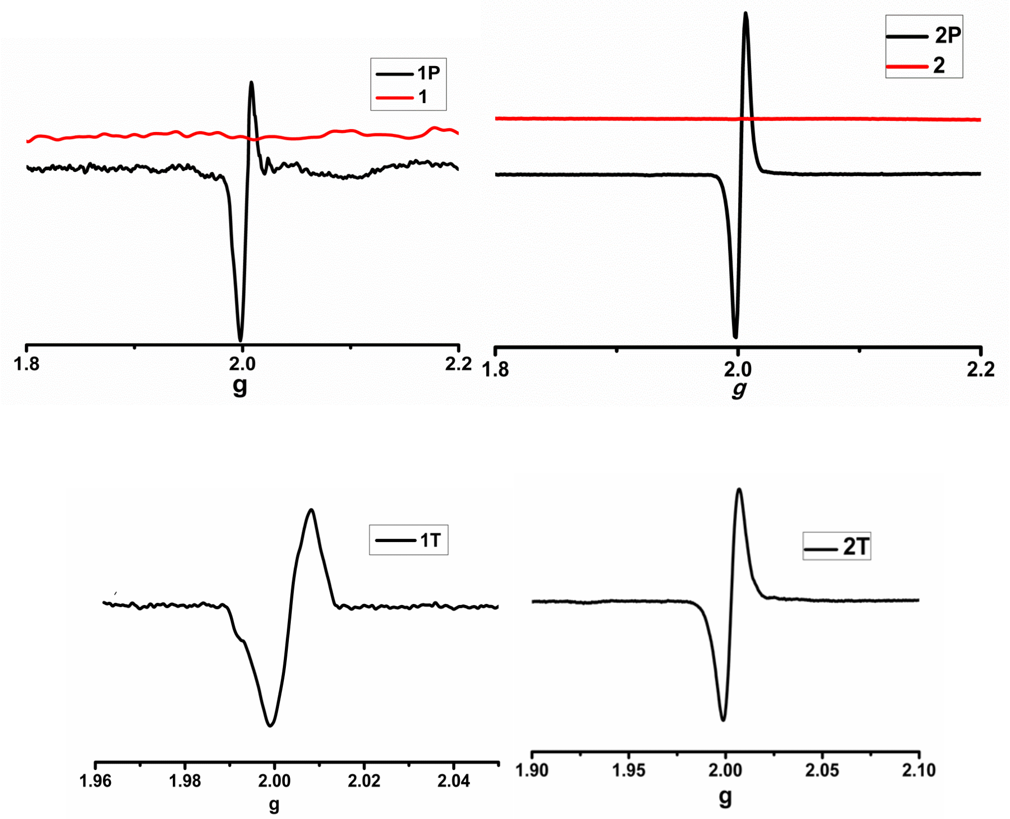

Fig. S3. ESR spectra for **1** and **2** before and after the photo or thermo effects.

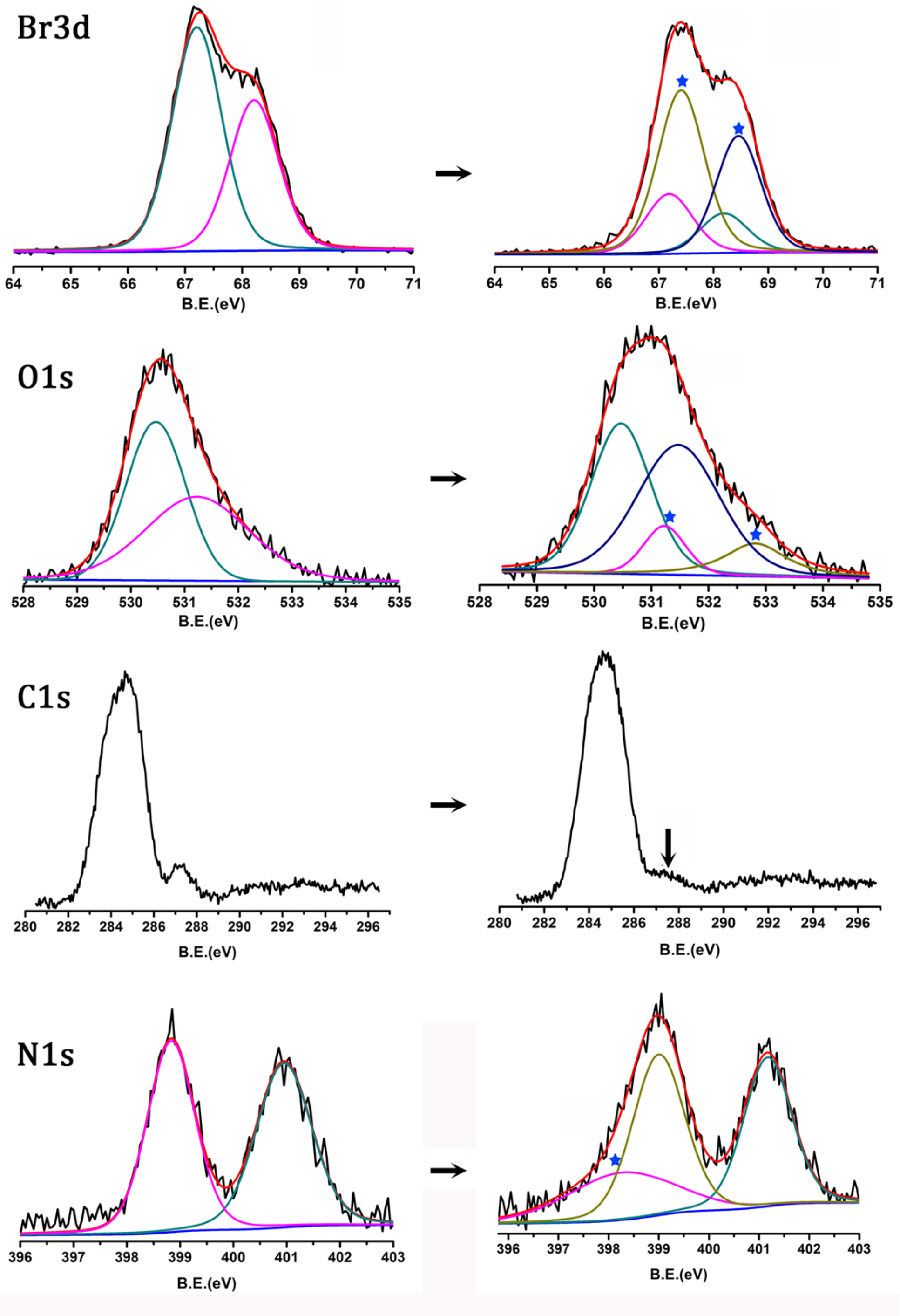

Fig. S4. XPS (Al-*K*α) core-level spectra of **2** (left) and **2T** (right). The new peaks were marked with stars and the variations were marked with arrows. The binding energies (B. E.) are in units of electron volts.

As shown in Fig. S4, the core-level spectra of Br 3d, O 1s, C 1s and N 1s varied remarkably after heating. There are two normal Br 3d5/2 and 3d3/2 peaks of the negatively charged Br atom, lying at around 67.19 and 68.19 eV, respectively, before heating. After heating for an hour, the two major Br 3d peaks became weak, and a new pair of prominent peaks centered at ~67.41 and 68.46 eV, respectively, appeared, suggesting that the Br atoms lost electrons. There are two types of O1s peaks laying at around 530.47 and 531.23 eV, respectively, before heating. After heating, the two major O 1s peaks became weak, and a new pair of prominent peaks centered at ~531.47 and 532.82 eV, respectively, appeared, suggesting that the O atoms also lost electrons. Therefore, the negatively charged Br and O atoms of **2** lost electrons and became neutral upon heating. Otherwise, the components of the neutral C and N atoms were prominently shifted to positions with lower binding energies. Hence, the thermochromism of **2** should originate from the electron transfer between the Br and O atoms and the 4,4'-bipyridinium moiety.

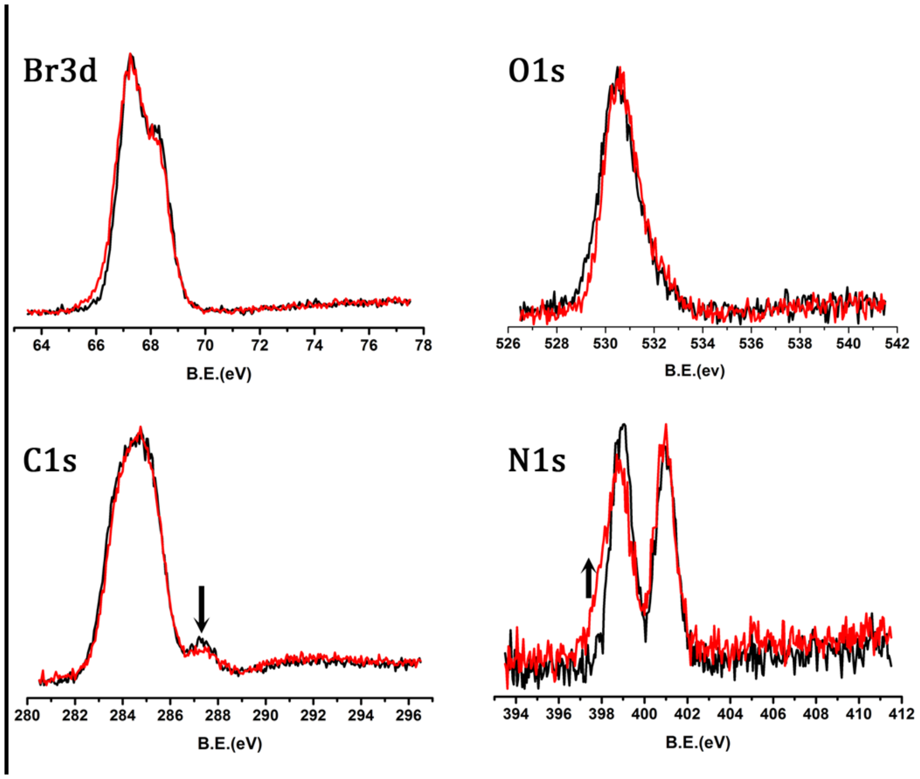

Fig. S5. XPS (Al-*K*α) core-level spectra of **2** (black line) and **2P** (red line). The variations were marked with arrows. The binding energies (B. E.) are in units of electron volts.

As shown in Fig. S5, the core-level spectra of Br 3d and O 1s hardly varied after irradiation, and the core-level spectra of C 1s and N 1s were slightly shifted to positions with lower binding energies after irradiation. On the whole, the variations were tiny.

Table S1. Crystal data and structural refinements for **1**, **1T**, **2** and **2T**.

Formula	$ZnCl_2C_{12}H_{16}N_2O_5$		$ZnBr_2C_{12}H_{16}N_2O_5$	
	1	**1T**	**2**	**2T**
Fw	350.49	350.49	439.41	439.41
Crystal system	monoclinic	monoclinic	monoclinic	monoclinic
Space group	*C*2/*c* (No. 14)	*C*2/*c*	*C*2/*c*	*C*2/c
a/Å	21.042(14)	21.004(9)	21.005(4)	20.940(13)
b/Å	8.881(5)	8.861(3)	9.1974(9)	9.168(4)
c/Å	16.352(10)	16.329(7)	16.531(3)	16.491(10)
β/°	113.670(9)	113.747(6)	114.679(8)	114.673(7)
V/Å^3	2798(3)	2781.9(19)	2901.9(8)	2877(3)
Z	8	8	8	8
D_c/g·cm^{-3}	1.664	1.674	2.012	2.029
μ (Mo $K\alpha$)/mm^{-1}	2.134	2.147	7.198	7.260
Goodness-of-fit on F^2	1.046	1.027	0.938	0.993
R_1, wR_2 [$I > 2\sigma(I)$]	0.0740, 0.2330	0.0733, 0.2273	0.0520, 0.1223	0.0642, 0.1662
R_1, wR_2 (all data)	0.0848, 0.2459	0.0852, 0.2416	0.0789, 0.1327	0.0848, 0.1800

$R_1 = \Sigma||F_o|-|F_c||/\Sigma|F_o|$, $wR_2 = \{\Sigma w[(F_o)^2-(F_c)^2]^2/\Sigma w[(F_o)^2]^2\}^{1/2}$.

Table S2. Selected bond lengths (Å) for **1, 1T, 2** and **2T**.

[Zn(CEbpy)$_2$Cl$_2$]					
	1	**1T**		**1**	**1T**
Zn(1)-O(1)	1.950(5)	1.952(4)	Zn(1)-N(1)	2.069(5)	2.062(5)
Zn(1)-Cl(3)	2.2841(17)	2.2794(16)	Zn(1)-Cl(2)	2.3129(17)	2.3086(16)
O(1)-C(12)	1.284(8)	1.270(8)	O(2)-C(12)	1.213(8)	1.213(8)
N(1)-C(1)	1.326(8)	1.326(8)	N(1)-C(3)	1.332(9)	1.327(9)

N(2)-C(8)	1.336(9)	1.336(8)	N(2)-C(10)	1.330(9)	1.333(9)
N(2)-C(11)	1.481(8)	1.480(8)	C(1)-C(2)	1.372(9)	1.371(9)
C(2)-C(5)	1.387(8)	1.385(8)	C(3)-C(4)	1.380(10)	1.376(10)
C(4)-C(5)	1.368(9)	1.363(10)	C(5)-C(6)	1.489(9)	1.484(8)
C(6)-C(7)	1.398(8)	1.402(9)	C(6)-C(9)	1.377(9)	1.371(9)
C(7)-C(8)	1.390(10)	1.378(10)	C(9)-C(10)	1.389(10)	1.376(11)
C(11)-C(12)	1.514(9)	1.518(9)			

[Zn(CEbpy)$_2$Br$_2$]					
	2	**2T**		**2**	**2T**
Zn(1)-O(2)	1.973(4)	1.967(4)	Zn(1)-N(1)	2.082(4)	2.074(5)
Zn(1)-Br(1)	2.398(1)	2.392(1)	Zn(1)-Br(2)	2.377(1)	2.374(1)
O(1)-C(12)	1.228(6)	1.217(7)	O(2)-C(12)	1.272(6)	1.278(7)
N(1)-C(1)	1.315(7)	1.308(8)	N(1)-C(3)	1.334(7)	1.333(8)
N(2)-C(8)	1.318(8)	1.318(8)	N(2)-C(10)	1.335(7)	1.321(8)
N(2)-C(11)	1.486(7)	1.472(7)	C(1)-C(2)	1.386(8)	1.385(9)
C(2)-C(5)	1.362(8)	1.377(9)	C(3)-C(4)	1.396(8)	1.382(9)
C(4)-C(5)	1.370(7)	1.362(8)	C(5)-C(6)	1.491(7)	1.480(8)
C(6)-C(7)	1.368(8)	1.370(9)	C(6)-C(9)	1.393(7)	1.377(8)
C(7)-C(8)	1.395(9)	1.396(7)	C(9)-C(10)	1.377(8)	1.383(9)
C(11)-C(12)	1.534(7)	1.532(8)			

Table S3. Comparison of bond lengths (Å) between **1** and **1T**.

[Zn(CEbpy)$_2$Cl$_2$]			
	1	**1T**	**Difference**
Zn(1)-N(1)	2.069(5)	2.062(5)	–0.004(5)
Zn(1)-Cl(2)	2.313(2)	2.309(2)	–0.004(2)
Zn(1)-Cl(3)	2.284(2)	2.279 (2)	–0.005(2)
O(1)-C(12)	1.284(8)	1.270(8)	–0.014(8)

N(2)-C(10)	1.330(9)	1.333(9)	+0.003(9)
N(2)-C(11)	1.481(8)	1.480(8)	–0.001(8)
C(2)-C(5)	1.387(8)	1.385(8)	–0.002(8)
C(3)-C(4)	1.380(10)	1.376(10)	–0.004(10)
C(5)-C(6)	1.489(9)	1.484(8)	–0.005(9)
C(6)-C(9)	1.377(9)	1.371(9)	–0.006(9)

Table S4. Comparison of bond lengths (Å) between **2** and **2T**.

[Zn(CEbpy)$_2$Br$_2$]			
	2	**2T**	**Difference**
Zn(1)-O(2)	1.973(4)	1.967(4)	–0.006(4)
Zn(1)-N(1)	2.082(4)	2.074(5)	–0.008(5)
Zn(1)-Br(1)	2.398(1)	2.392(1)	–0.006(1)
Zn(1)-Br(2)	2.377(1)	2.374(1)	–0.003(1)
O(1)-C(12)	1.228(6)	1.217(7)	–0.011(7)
N(2)-C(10)	1.335(7)	1.321(8)	–0.014(8)
N(2)-C(11)	1.486(7)	1.472(7)	–0.014(7)
C(2)-C(5)	1.362(8)	1.377(9)	+0.015(9)
C(3)-C(4)	1.396(8)	1.382(9)	–0.014(9)
C(5)-C(6)	1.491(7)	1.480(8)	–0.011(8)
C(6)-C(9)	1.393(7)	1.377(8)	–0.016(8)

References:

1. A. D. Phillips, Z. F. Fei, W. H. Ang, R. Scopelliti and P. J. Dyson, *CrystEngComm*, 2009, **9**, 1966
2. *CrystalClear*, version 1.3.5; Rigaku Corp.: The Woodlands, TX, 1999.
3. (a) G. M. Sheldrick, *SHELXTL*, version 5.1; Bruker-AXS: Madison, WI, 1998; (b) *SHELXTL^{TM} Version 5* Reference Manual; Siemens Energy & Automation Inc.: Madison, WI, 1994.